Rapid inactivation of airborne porcine reproductive and respiratory syndrome (PRRS) virus using an atmospheric pressure air plasma

Gaurav Nayak[1], Austin J Andrews[1], Ian Marabella[1], Hamada A Aboubakr[2], Sagar M Goyal[2], Bernard A Olson[1], Montserrat Torremorell[3] and Peter J Bruggeman[1]*

[1]Department of Mechanical Engineering, University of Minnesota, Minneapolis, Minnesota 55455, USA

[2]Department of Veterinary Population Medicine and Veterinary Diagnostic Laboratory, College of Veterinary Medicine, University of Minnesota, St. Paul, Minnesota 55108, USA

[3]Department of Veterinary Population Medicine, College of Veterinary Medicine, University of Minnesota, St. Paul, Minnesota 55108, USA

E-mail: nayak025@umn.edu, pbruggem@umn.edu

February 2020

Abstract. The transmission of airborne diseases in animals poses great risks to animal safety with potential significant economic losses. In this study, we report on the use of a dielectric barrier discharge (DBD) for in-flight inactivation of airborne aerosolized porcine reproductive and respiratory syndrome (PRRS) virus. The infectivity of the sampled virus downstream compared to upstream of the DBD reactor as determined by the $TCID_{50}$ method showed a $\sim$3.5 $\log_{10}$ reduction in the virus titer. Independent testing of the viral genome by the RT-qPCR method confirmed the inactivation with minimal filtering effects. Both short-lived species such as $^{\cdot}OH$ and $O_2(a^1\Delta_g)$ and peroxynitrous acid (ONOOH) chemistry at low pH in the virus-laden droplets are suggested to be responsible for the observed inactivation.

Keywords: airborne, dielectric barrier discharge, inactivation, porcine reproductive and respiratory syndrome, reactive species

1. Introduction

The transmission of infectious airborne diseases and related outbreaks in animals have been a major global concern causing severe economic and sociopolitical disruption.[1–4] These diseases can spread among animals via direct contact with an infected source or transport of infectious aerosols across short distance from the source to the receptor.[5,6] The situation becomes challenging in livestock and poultry farms containing dense populations of pigs or avian species, where local spread of diseases can be difficult to contain.[7] These include economically important pathogens such as porcine reproductive and respiratory syndrome (PRRS) virus and influenza A virus in pigs, and Newcastle disease virus and avian influenza virus (AIV) in poultry.[2,7] For example, Neumann et al estimated the total annual economic impact of the 2005 PRRS outbreaks on US swine producers at USD 560 million.[2] Similarly, in 2015, the turkey industry in Minnesota experienced an unprecedented outbreak of highly pathogenic AIV, leading to euthanasia of nearly 4.8 million turkeys and a total direct loss of $1.6 billion due to the outbreak.[3]

Many excellent surveillance programs have been implemented on farms.[8,9] However, efficient and cost-effective preventive measures are yet to be implemented. Bio-security and bio-containment measures only limit the introduction of airborne pathogens into the animal containment zones by avoiding direct contact between animals and infected source(s), thus minimizing herd-to-herd transmission.

Nonetheless, aerosol transmission can occur over larger distances.[10,11] Recent field evidence suggests that PRRS, swine flu (H1N1) and avian flu (H5N2) viruses can be transmitted by wind from a positive source to unaffected farms.[12–14] For instance, PRRS virus RNA was detected up to 9.1 km away, downwind from the infected source populations.[12] The same study also showed that PRRS virus can remain infectious for 4.7 km away from an infected herd.[12] This is due to the spread of virus aerosols to the

neighboring farms and their livestock. The stability of PRRS virus in the environment over long distances occurs due to low environmental temperature and/or low relative humidity.[15] It has been shown that the PRRS outbreaks follow a seasonal pattern in the Midwest of the United States, with an onset in the month of October signifying cold and damp weather conditions.[16]

Despite these alarming statistics, the importance of airborne disease transmission and corresponding mitigation technologies are underrated compared to their counterparts (water, soil, food or arthropod-mediated infections). The most common mitigation technique is the use of filters such as MERV (minimum efficiency reporting value) 14 or 16 in the HVAC systems. These filters are currently used at some swine barns, but the effectiveness of such filters diminishes with a reduction in the particle size (<0.3 μm).[17] The particle removal efficiency of such filters depends on various factors such as the particle size, face velocity, and resistance to airflow through the filter media, which in turn, are affected significantly by the particle or dust loading over time. Furthermore, if the filter chamber is not sealed properly, the untreated air simply enters indoor spaces at partial vacuum. Prolonged use of such filters leads to growth of microorganisms on HVAC filters, which can then be released back into the air. Moreover, the virus can remain active when trapped in the filter.[18] The cost of running these filters is high, as they need replacement every 12 to 18 months due to loading.

Ultraviolet germicidal irradiation (UVGI) is another commonly employed air-cleaning technology. Most commercially available UVGI systems use low-pressure mercury vapor lamps that emit radiation at 253.7 nm as a source of UV-C radiation. UV radiation is known to be effective in killing or inactivating *Feline calicivirus* (FCV), hepatitis A virus, echovirus 12, MS2 bacteriophage, poliovirus, adenovirus and many others on surfaces or in liquids.[19–22] Significant research has also been carried out to inactivate airborne pathogens using UVGI systems.[23–26] The modern UV air disinfection techniques are applied as either in-duct irradiation (airstream and surface

disinfection) or upper-room UVGI to inactivate airborne pathogens.[27] In-duct UV irradiation reduces the viability of the microorganisms as they flow through the HVAC systems and prevents the growth of microorganisms on cooling coils or inactivates bacteria and viruses captured on the filter surfaces inside HVAC systems.[25,27] In airstream disinfection, the potential to inactivate pathogens is little owing to small particle residence times in a single pass system.[25–27] Moreover, pathogens shielded from the direct UV exposure (inside filter media, porous insulation or fibrous material liners) are difficult to inactivate.[25] It has also been shown that many viruses use the repair enzymes of the host cells to revive their genome after UV irradiation via dark repair or photo-reactivation.[28,29] The US EPA concludes that there are no standard test procedures to assess the effectiveness of UVGI systems and there is not enough evidence to suggest that UVGI provides any additional protection over the use of conventional HEPA filtration alone.[18]

Other mitigation techniques include electrostatic precipitators (ESPs), which uses a high voltage wire to charge incoming particles by inducing a corona discharge. Electrically charged air molecules produce negative ions that attach to the airborne particles. The charged airborne particles are collected onto oppositely charged plates inside air cleaners. Most ESPs have a single-pass removal efficiency of 60% and can reach up to a maximum of 95% with the use of clean ESPs.[30] However, the efficiency of ESPs decreases with increase in particle loading and they require regular cleaning to retain their efficiency.[31,32]

Finally, some non-conventional air-disinfection technologies to inactivate bio-aerosols include carbon nanotube filter and photo-catalytic oxidation.[33–35] Newer techniques such as thermal treatment[36,37] and microwave irradiation[38,39] have also been investigated for the inactivation of airborne pathogens. Due to lower bio-aerosol removal efficiencies and/or large energy consumption, many of these techniques have not been studied in detail.

In recent years, non-thermal plasmas operated at atmospheric pressure have gained

increased attention as highly effective and alternative technology for inactivation of microbial agents or pathogens.[40–45] Due to the associated electric field, non-thermal plasmas can alter particle transport by inducing negative charge on the particles, thus imparting charge-driven filtration as well as trapping of these particles. This process is similar to an ESP and can enhance conventional filtration processes when used in series with existing HEPA filters.[46] Since non-equilibrium plasmas operated in air produce a cocktail of reactive oxygen and nitrogen species or RONS (O_3, $O_2(a^1\Delta_g)$, NO, NO_2, N_2O_5, HNO_2, HNO_3, $ONOO^-$, H_2O_2, $^{\cdot}OH$ and many other reactive species),[47] they can react with the airborne particles and mediate various oxidative processes. Thus, plasma can simultaneously act as a particle filter as well as a disinfection technology.

Although plasmas have been extensively investigated for the inactivation of liquid, food and surface-borne pathogens,[48–57] only a handful of studies showing inactivation efficacy of plasmas against airborne pathogens have been conducted, and even less, concerning airborne viruses.[58,59] Previously, the use of cold oxygen plasma in a single-pass flow tunnel resulted in 3.1, 2 and 2.1 $\log_{10}$ $TCID_{50}$/ml reduction in human parainfluenza virus type 3 (hPIV-3), respiratory syncytial virus (RSV) and influenza virus A (H5N2) titers, respectively.[60] In another study, >95% inactivation of aerosolized MS2 bacteriophage was achieved in ambient air with a plasma power and exposure of 28 W and 0.12 s, respectively.[59] Recently, Xia et al reported >2.3 $\log_{10}$ reduction in the infectivity of MS2 bacteriophage using a packed-bed non-thermal plasma reactor at airflow rate of 170 standard liters per minute (slm).[58]

Different research groups have proposed several mechanisms for inactivation of viruses by atmospheric pressure non-thermal plasmas. Ozone (O_3) has been one of the most suggested contenders among many researchers for inactivation of viruses[61–63] although RNS has also been shown to be effective.[51] Zimmermann et al reported that the inactivation of adenovirus in solution was mainly due to the dissolved RONS using a surface dielectric barrier discharge (DBD).[57] Recently, Aboubakr et al reported on inactivation of FCV in liquid using radio-frequency plasma jet and concluded that the

inactivation was achieved by two distinct pathways: $O_2(a^1\Delta_g)/O_3$-mediated inactivation in the presence of O_2, and peroxynitrous acid (ONOOH)-based inactivation in the presence of air.[50] Proteomics studies suggest that the impact of plasma occurred through oxidation of the virus capsid.[50] In our previous work, a 5 $\log_{10}$ reduction in viable FCV titer coated on stainless steel surface was achieved within 3 minutes of plasma treatment using a two-dimensional flow-through DBD reactor in air. It was concluded that both O_3 and RNS contributed to the observed inactivation effect.[51]

The most important challenge in virus inactivation in HVAC system is the requirement to inactivate airborne virus particles with a plasma contact time similar to the gas residence time of ∼10 milliseconds (ms) for typical airflows in HVAC systems. It is hypothesized that the highly efficient reactivity transport of short-lived reactive species from plasma to the aerosolized virus particles could lead to efficient oxidative processes that underpin the virus inactivation.

In this study, we report for the first time the successful inactivation of an economically important pathogen (PRRS virus) using the novel technique of electrical discharges without the addition of any environmentally harmful chemicals. The aerosolized virus particles encapsulated within sub-micron-sized liquid droplets are sent through a plasma reactor at high input airflow rate in an aerosol test tunnel, which provides a particle residence time of only a few milliseconds within the plasma. We used a volumetric or planar-type DBD as it can sustain high airflow rate due to the negligible pressure drop across the reactor, and can simultaneously treat large volume of air. The strong micro-discharges can generate moderate electron density to initiate electron-impact reactions required to produce high concentration of chemically active species. It also eliminates the necessity of frequent maintenance as it minimizes clogging of liquid and virus particles within the reactor, unlike packed-bed DBD reactors. The used DBD reactor has previously been successfully used in the exhaust treatment of marine diesel engines at low temperature conditions.[64] The prototype of such a rapid in-flight inactivation approach has the potential to be integrated into existing commercial

HVAC units used in swine or poultry farms.

2. Experimental Section

2.1. Experimental setup, plasma reactor and operation parameters

The experimental setup is shown in **Figure 1** and includes a small-scale single-pass aerosol/wind tunnel and a volumetric DBD reactor. The cylindrical wind tunnel is made of clear polycarbonate and has an inside duct diameter of 8.9 cm and an effective length of 4 m. The wind tunnel is designed to operate in a volumetric flow rate range of 85 to 850 slm. A vacuum blower (SFEG, BBA14-111HEB-00, 5.25 A, 120 V) at the outlet of the tunnel draws ambient air (25–28% RH) into the duct through a HEPA filter (AstroCel II, American Air Filter) to prevent entry of particles suspended in the ambient air. Another HEPA filter is mounted at the outlet of the tunnel just before the vacuum blower to prevent release of PRRS virus aerosols introduced in the wind tunnel into the ambient air. A calibrated flow orifice meter is mounted inside the tunnel at the exit, across which the pressure drop is measured using an electronic differential pressure transducer (Ashcroft CXLdp 0.1" Water, ±0.25%). Temperature and relative humidity of the air and absolute pressure inside the tunnel are also measured operando using suitable sensors (Omega HX402). The pressure drop is fed into a PID feedback control in LabVIEW software, which applies a necessary voltage to the motor of the vacuum blower to control and maintain a desired volumetric airflow rate. LabVIEW uses a National Instruments USB-6001 DAQ to facilitate data acquisition.

The aerosol generator is a ∼0.2 mm (0.008") nozzle nebulizer (Altech) and is installed at the inlet of the wind tunnel. The buffered PRRS virus solution is fed to the nebulizer from a 65 ml syringe at a constant liquid feed rate of 3 ml/min using an electronic syringe pump. The virus solution is aerosolized while leaving the nebulizer nozzle on shearing action by feeding dry and filtered air to the nebulizer at a volumetric flow rate of around 1 slm through a rotameter. Additionally, dry and compressed air

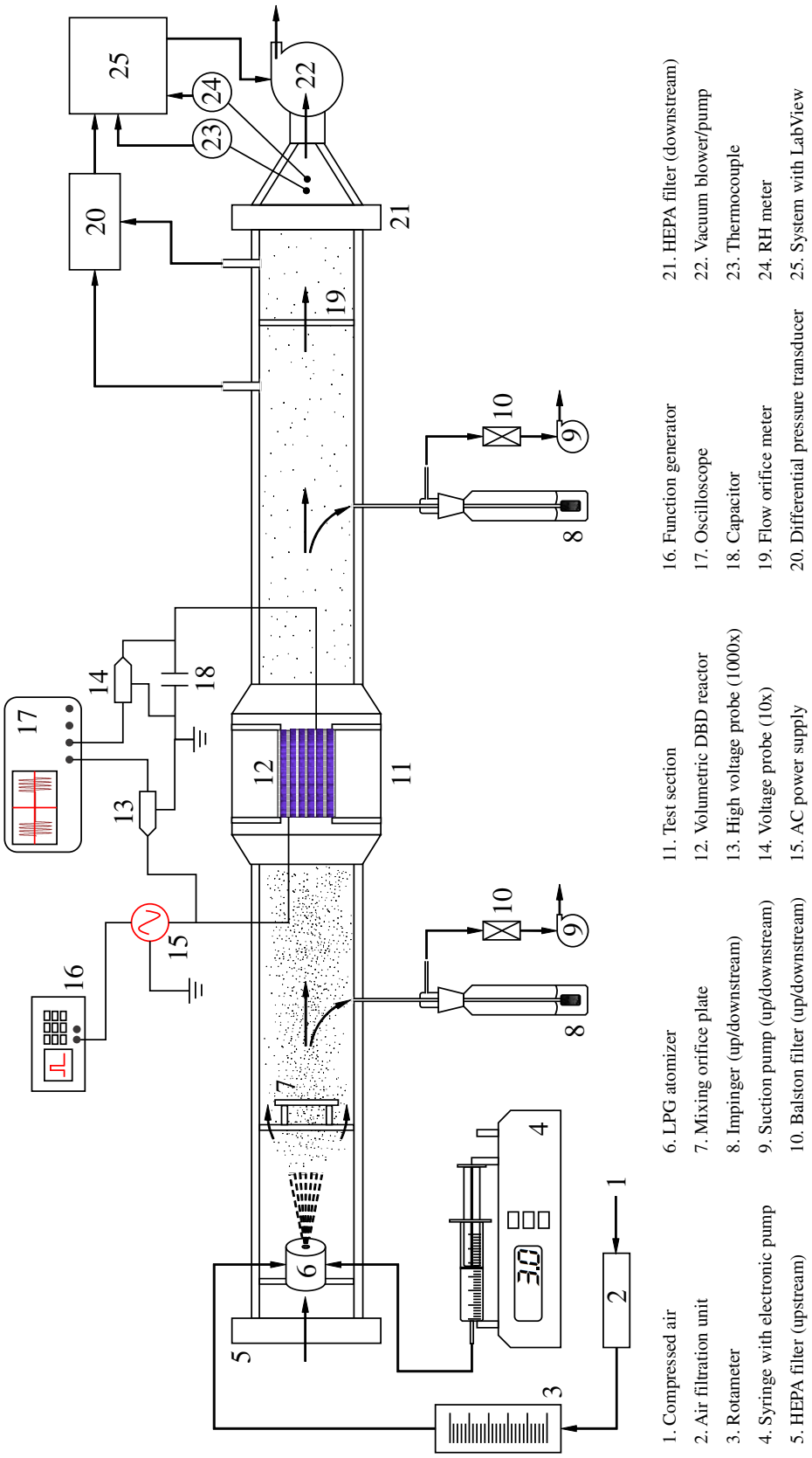

Figure 1. Experimental setup.

from the building facility is fed into the tunnel at a flow rate of 80–90 slm to further enhance aerosol generation and to dry and dilute PRRS virus aerosols upon entering the tunnel. A mixing baffle located inside the tunnel after the nebulizer creates turbulence that thoroughly mixes the aerosols. The long tunnel facilitates a fully developed flow, thus creating a homogeneous concentration of aerosols in the tunnel. Isokinetic probes are located upstream and downstream of the plasma reactor to connect to a portable optical particle counter (OPC, AeroTrak 9306-V2, TSI Inc.) via an aerosol diluter to determine particle concentrations. Aerosol/air sampling is done by drawing air through the isokinetic probes into the impingers containing a solution depending on the experiment as described before, located both upstream and downstream operating at flow rates of around 9 slm (measured by a gilibrator from Sensidyne Gillian) using suction pumps.

The schematic of the flow-through volumetric DBD reactor used in this study is shown in **Figure 2**. The DBD reactor consists of seven thin metallic plate electrodes (high voltage and grounded) arranged in an alternating pattern and are separated and covered by alumina as the dielectric material. This results into six rectangular slits corresponding to the active discharge zones. This electrode arrangement is embedded in a holder made of polytetrafluoroethylene (PTFE), with provision for high voltage and ground electrical connections. The DBD reactor is mounted inside the test section of the wind tunnel and sealed using a rubber gasket to prevent infiltration of untreated air downstream of the test section.

The discharge is ignited in the rectangular slits by a high voltage sinusoidal signal with a frequency in the range of 26–29 kHz generated by an AC power source (PVM500). The signal is modulated at a 1 kHz modulation frequency with a duty cycle of 12.5, 25 or 50% using a function generator (Tektronix AFG3022B). This modulation allows to operate the discharge at different average power levels for fixed instantaneous plasma power. The applied voltage varies in the range of 12.9 to 14.9 kV. The applied voltage (V) was measured using a high-voltage probe (Tektronix P6015A) and the charge (Q)

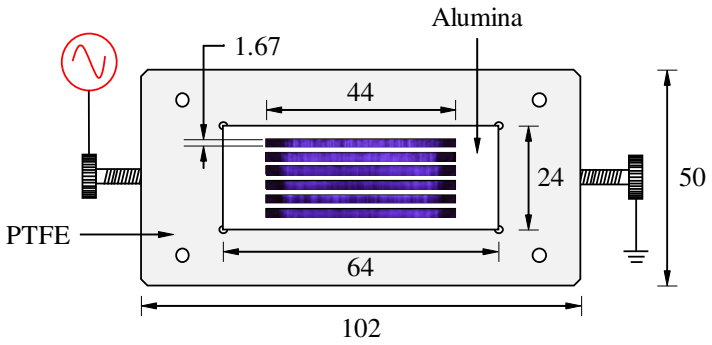

Figure 2. Cross-section of the DBD reactor used in this study. The length of the reactor is 68 mm. Note that all dimensions in the figure are in mm.

was obtained by measuring the voltage V_C across a capacitor (C) of 100 nF in series with the plasma reactor, using a general-purpose passive voltage probe (Tektronix TPP0200). The corresponding waveforms were recorded by a digital oscilloscope (Tektronix DPO2024B, 200 MHz, 1 GS s^{-1}). The power dissipated in the discharge (P) is calculated from the voltage-charge (Lissajous) plots using the following equation [65]

$$P = fD \int_T V \, \mathrm{d}Q = fDC \int_T V \, \mathrm{d}V_C \tag{1}$$

where T is the discharge period of the AC voltage, f the frequency and D the duty cycle. The current is indirectly obtained by measuring the charge across the capacitor and differentiating it with respect to time.

2.2. Propagation of PRRS virus

The PRRS virus (strain VR2332) was propagated in monkey kidney cells (Marc-145). Monolayers of Marc-145 were grown in 175 cm^2 cell culture flasks using minimum essential medium (MEM) containing Earle's salts and L-Glutamine (Mediatech Inc., Manassas, VA, USA) and supplemented with 8% fetal bovine serum (FBS) and antibiotics (neomycin (90 U ml^{-1}), gentamicin (50 μg ml^{-1}), penicillin (455 IU ml^{-1}), streptomycin (455 μg ml^{-1}), and fungizone (1.5 μg ml^{-1})). Marc-145 monolayer flasks with $\geq$80% confluence were infected by PRRS virus suspension at 0.1 multiplicity of infection. The flasks were then incubated at 37°C in a 5% CO_2 incubator for 3–5 days

until cytopathic effects (CPE) appeared when examined under an inverted microscope. The virus was harvested by freezing and thawing only once followed by centrifugation at 3000×g for 15 minutes at 4°C to get rid of the cellular debris. The cell free supernatant containing the virus (10^5 $TCID_{50}$ ml^{-1}) was aliquoted and stored at −80°C until further use.

2.3. Experimental procedure

Before running each test, the vacuum blower and the DBD reactor were switched on for 5 minutes to stabilize the airflow rate as well as the reactive species concentrations inside the tunnel. During the experiment, the temperature and relative humidity of the air being drawn inside the wind tunnel was in the range of 21–24°C and 25–28%, respectively. The volumetric airflow rate inside the wind tunnel was fixed at 109 ± 5 slm at a maximum pressure drop of 45 Pa across the DBD reactor. For each experiment, a 65 ml syringe was filled with an appropriate volume of PRRS virus solution with an initial titer of 5.5 $\log_{10}$ $TCID_{50}$ ml^{-1} and fed to the nebulizer at a constant feed rate of 3 ml min^{-1} by switching on the syringe pump. Electric suction pumps connected to each of the impingers via filters (Balston BKU) were turned on to draw samples from the air at a nominal flow rate of 9 slm. The air stream in the tunnel seeded with aerosolized PRRS virus was sampled upstream and downstream of the DBD reactor for sampling times of 5 and 10 minutes. The air samples were collected in impingers containing 18 ml of DMEM solution. After 5 and 10 minutes of sampling, the discharge and suction pumps connected to the impingers were turned off and the volume of liquid in each of the impingers was measured, recorded and aliquoted into 15 ml conical centrifuge tubes (Falcon). The surviving virus samples were titrated right after collecting the samples, aliquoted and frozen at −80°C for genome quantification. Virus samples were also collected just before the nebulizer to serve as the reference or standard.

Infectivity assays ($TCID_{50}$) and RT-qPCR assays were performed on each sample to quantify the concentration of infectious virus ($TCID_{50}$ ml^{-1}) and the total (both infective

and inactivated) concentration of PRRS virus genome copies per milliliter of solution (gc ml^{-1}) in the collecting liquid, respectively. Both of these methods are described in detail in the subsequent sections. The virus experiments were performed at sampling times of 5 and 10 minutes for three different power levels of 37 ± 1, 79 ± 3 and 129 ± 2 W. The control experiments were performed with the reactor turned off in duplicates, while the experiments with the reactor turned on were performed in triplicates.

Since O_3 or other reactive species produced from the DBD reactor are able to dissolve into the sampling liquid in the downstream impinger due to strong mixing, and inactivate PRRS virus during and after sample collection, 2 ml of 2 M sodium thiosulfate ($Na_2S_2O_3.5H_2O$) was added to the DMEM solution in up and downstream impingers to quench all the oxidizing species in the solution. The effect of the concentration of sodium thiosulfate (2 M) on PRRS virus was determined pre-treatment by adding different concentrations of sodium thiosulfate ranging from 2 mM to 2 M into DMEM solution containing PRRS virus in a petri dish and quantifying the viability of the virus at different times (10 min, 30 min, 1 h and 2 h). The result shown in **Figure 3** for $Na_2S_2O_3$ (2 ml of 2 M scavenger added to 18 ml DMEM solution containing PRRS virus and exposed for a period of 2 h) confirmed that even the highest concentration and exposure period did not have any impact on the viability of the virus titer. DMEM solution without PRRS virus was aerosolized and sent through the DBD reactor with the discharge ignited at 129 W and sampled for 2.5, 5 and 10 minutes into the up and downstream impingers containing 18 ml of collection liquid with PRRS virus solution and 2 ml of 2 M sodium thiosulfate along with the control tests with no plasma. The difference in the virus titers of the scavenger experiment in petri dish (shown in pink and green bars) and the control (shown in red bar) is because the initial titer of the virus for these two experiments were different and the experiments were performed on different days. Figure 3 shows that the concentration of sodium thiosulfate was sufficient to quench all dissolved reactive species and had no significant impact on the suspended virus in the impinger. This confirms that any further inactivation that would occur

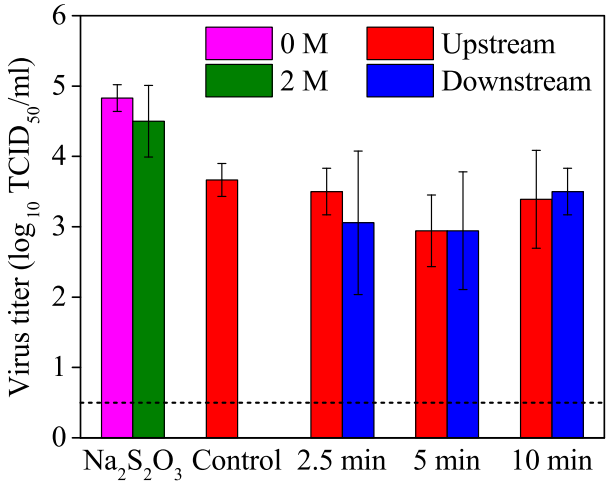

Figure 3. Positive control test to assess the effect of 2 M sodium thiosulfate on PRRS virus titer for an exposure period of 0 and 2 hours (shown in pink and green bars), and to show the ability of 2 M sodium thiosulfate to scavenge RONS produced by the plasma in the impinger for a treatment time of 2.5, 5 and 10 minutes (shown in red and blue bars).

during the plasma-aided treatment of the aerosolized virus will be due to the impact of plasma-produced reactive species on the virus in the gas phase.

2.4. Virus titration and quantification

2.4.1. Tissue culture infective dose ($TCID_{50}$) method for PRRS virus infectivity titration

Infectivity of PRRS virus was titrated by the end-point technique to determine the 50% tissue culture infectious dose ($TCID_{50}$), in which, serial 10-fold dilutions of all samples were prepared in MEM containing 4% fetal bovine serum (FBS). Aliquots (100 μl) of each sample dilution were used to infect three wells of Marc-145 cell monolayer (5–7 day old) pre-prepared in 96-well cell culture microtiter plates. The plates were incubated at 37°C and 85% relative humidity in a 5% CO_2 incubator and were examined daily for the development of cytopathic effects (CPEs) for up to 5 days. The highest dilution of the virus, which produced CPE in 50% of the infected cells, was considered as the endpoint. The titer of the surviving virus in each sample was calculated by using the

Spearman-Kärber method and expressed as the logarithmic value of 50% tissue culture infective doses per ml ($\log_{10}$ $TCID_{50}$ ml^{-1}) of eluted virus suspension.[66]

2.4.2. Reverse transcription quantitative real-time polymerase chain reaction (RT-qPCR) for titration of PRRS virus genome copies Viral RNA was isolated from 50 μl aliquots of each sample using Ambion MagMAX^{TM}–96 Viral Isolation Kit (ThermoFisher Scientific, MA) employing magnetic beads in an automated process using KingFisher Flex instrument (ThermoFisher Scientific, MA). The viral RNA was obtained in 50 μl elution buffer and kept at -80°C in the freezer until further use in PCR determination.

The RT-qPCR was performed on isolated viral RNA using and following the protocol provided by the commercially available VetMAX^{TM}NA and EU PRRSV and Xeno^{TM}RNA Controls diagnostic kit (Applied Biosystems, CA). Two primer sets and two TaqMan probes for quantification of PRRS virus were provided in a mix reagent with proprietary information. The probe for EU strain is attached with CF560 and BHQ-1 dyes, as reporter and quencher, respectively. However, the probe for NA strain is attached with FAM^{TM}and BHQ-1 dyes, as reporter and quencher, respectively. In this work, NA PRRSV strain was used, so, a singleplex RT-qPCR was run by measuring the signal of FAM^{TM}only. Each RT-qPCR reaction mixture was comprised of 12.5 μl of 2x Multiplex RT-PCR buffer, 2.5 μl of PRRSV primer probe mix V2, 2.5 μl of Multiplex enzyme mix, 0.5 μl of nuclease-free water and 7 μl of template RNA to have a final volume of 25 μl. Real-time PCR was performed in ThermoFisher Scientific Applied BioSystems Quantstudio-5 Real-Time PCR thermocycler system under the following thermocycling conditions: reverse transcription at 48°C for 10 min; Taq polymerase activation at 95°C for 10 min; 40 amplification cycles each for denaturation step at 97°C for 2 s and an annealing step at 60°C for 40 s. Fluorescence was measured at the end of the annealing step in each cycle.

For accurate quantification of PRRS virus RNA, PRRSV-RNA standards/calibration

curve was constructed as described previously with another virus, in which a standard cDNA transcript of open reading frame (ORF6) of PRRSV NA genome was used.[67] This included the targeted sequence of the PCR primers. In RNase-free water, 10-folds serial dilution was prepared using viral RNA extracted from 50 μl of PRRS virus with known $TCID_{50}$ ml^{-1} titer. The standard curve translated the cycle threshold (Ct) values into viral RNA copy number equivalents expressed as ($\log_{10}$ copy viral genome ml^{-1}). The standard curve was generated from average Ct values of three measurements per dilution. At each RT-qPCR measurement, a standard curve was generated under the same conditions as the tested samples.

2.5. pH measurements

The pH was measured for each aliquoted sample without the virus (both control and plasma-treated) in the up- and downstream using a pH probe (Thermo Fisher Scientific Orion, 8220BNWP, Waltham, MA, USA).

2.6. O_3 *densities*

The gas-phase absolute ozone (O_3) density could not be measured during all the testing conditions as the quartz windows were repeatedly covered with condensation from large concentration of aerosols. However, the measurements were performed without aerosols for the same plasma settings, airflow rate, relative humidity and temperature as the actual testing. The absolute O_3 density was measured 30 cm away from the discharge by UV absorption spectroscopy using a mercury-argon lamp as a source of radiation at 254 nm and a low-resolution spectrometer (Avantes AvaSpec-2048) as the detector. The measurement technique and the analysis using Beer-Lambert's law are described in detail previously.[68] This approach yields an upper limit of the O_3 density in the gas phase.

2.7. H_2O_2 *concentration*

The concentration of H_2O_2 in the sampled liquid was measured by using the colorimetric method described by Eisenberg.[69] 300 μl were extracted from the sampled liquid after plasma treatment and distributed equally into three wells of a 96-well microtiter plate. 13.3 μl of 10 mM sodium azide (NaN_3) solution was immediately added to each of these 100 μl samples to quench the reactive nitrogen species that could react with H_2O_2. Next, 100 μl of titanium oxysulfate ($TiOSO_4$) was added to each of these wells. The resulting solution was transferred to a micro-cuvette and the absorbance was determined at 405 nm by measuring the intensity of the transmitted light through the solution using a broadband spectrometer (Avantes AvaSpec-2048) and an LED (M405LP1, Thorlabs) as the light source. The absorbance was calibrated with known concentrations of standard H_2O_2 solution ranging from 100 to 1000 μM. The experiments were repeated three times.

2.8. NO_2^- *and* NO_3^- *concentrations*

The dissolved nitrite (NO_2^-) and nitrate (NO_3^-) concentrations were measured by absorption spectroscopy using Griess assay, based on the method described by Miranda et al.[70] Equal volumes of 0.1% of N-(1-naphthyl) ethylenediamine dihydrochloride (1 mg ml^{-1}) solution and 1% of sulfanilic acid (10 mg ml^{-1}) solution in 5% phosphoric acid present in the Griess Reagent Kit (G-7921, Molecular Probes) were mixed with minimum exposure to light to prepare the Griess reagent. Since this method can only quantify nitrites, the nitrates in the solution need to be reduced to nitrites. This was achieved by using vanadium (III) chloride (VCl_3), which was prepared by adding 400 mg of solid VCl_3 to 50 ml of 1 M HCl. These measurements were performed by aerosolizing DMEM solution without any suspended PRRS virus with the plasma turned on and by sampling only at the downstream in the impinger containing 20 ml of distilled water. After 5 and 10 minutes of sampling, 600 μl were extracted from the sampled liquid in the impinger by a pipette and distributed equally into six wells of a 96-well microtiter plate (3 each for net and gross nitrite quantification). The production of nitrates from nitrites

in the acidic environment was stopped by adding 10 μl of homemade buffer solution (pH 8.0 ± 0.2). However, in the absence of sodium thiosulfate, the conversion of nitrites to nitrates by O_3-induced oxidation cannot be suppressed by the addition of buffer only. 10 μl of sodium pyruvate was added to each of the treated sample to scavenge any possible traces of the plasma-produced H_2O_2, as this might also affect the Griess assay. Finally, 20 μl of Griess reagent was added to 100 μl of each of the treated sample after the addition of 80 μl of either deionized (DI) water (for net nitrite concentration) or prepared VCl_3 solution (for converting nitrate to nitrite and quantifying the gross nitrite concentration). The difference between the gross and net nitrite concentrations provides the net nitrate concentration.

A reference sample or control was prepared by following the above protocol but using 100 μl of DI water instead of the sampled liquid. The samples for net and gross nitrite quantification were incubated at room temperature and at 37°C for 30 minutes, respectively. The samples were then transferred into a micro-cuvette and the absorbance was determined at 565 nm by measuring the intensity of the transmitted light through the sample using a broadband spectrometer (Avantes AvaSpec-2048) and an LED (M565L3, Thorlabs) as the light source. The absorbance was calibrated with known concentrations of standard sodium nitrite solutions (10–100 μM). For samples with nitrite concentrations higher than 100 μM, the samples were diluted with DI water to avoid saturation of the absorbance. These experiments were repeated thrice for each sampling time.

3. Results and Discussion

3.1. Plasma and flow characterization

The current and voltage waveforms of the discharge are shown in **Figure 4(a)** at the highest discharge power used in this study. The corresponding power dissipated in the discharge during the modulation period of 1 kHz and a duty cycle of 50% is also shown.

The steady-state power is determined to be 260 W, while the time-averaged power dissipated is 129 W. A zoomed in section of typical voltage and current waveforms are shown in **Figure 4(b)**. The applied peak-to-peak voltage is 12.3 kV corresponding with a current of ∼0.4 A. The multiple peaks in the current waveform is consistent with multiple micro-discharge activity in the positive and negative halves of a discharge cycle. The current waveform for each cycle in Figure 4(b) consists of two periods of discharge activities with a duration of ∼12 μs. Similarly, using duty cycles of 12.5 and 25% for the same power supply settings, time-averaged power levels of 37 and 79 W were obtained, respectively. The volumetric airflow rate inside the wind tunnel (109 slm) was measured at the location of the calibrated orifice meter, located in the downstream region close to the outlet of the wind tunnel. Considering the loss of flow during the operation of the impinger in the downstream region, the actual flow rate through the DBD reactor is 9 slm larger and around 118 ± 5 slm. At this flow rate, the specific energy density in the plasma for the investigated operating conditions ranges from 19 to 66 J l^{-1}. Considering the volume and the volumetric flow rate, the gas residence time in the plasma is ∼15 ms. Since the plasma is operated in modulated mode, the virus aerosols remain in direct contact with the active discharge zone for 1.9, 3.8 and 7.5 ms for a duty cycle of 12.5, 25 and 50%, respectively. However, the aerosols remain in contact with the plasma effluent for ∼3 s before being collected in the downstream impinger, which is more than 1 order of magnitude shorter than the time required for complete surface decontamination using a remote two-dimensional DBD reactor.[51]

The maximum increase in the gas temperature, ΔT [K] corresponding to the flow rate of 118 slm can be estimated from a thermal balance assuming that all heat is removed through forced convection by the airflow as follows:

$$\Delta T = \frac{P}{QC_{\mathrm{p}}\rho} \tag{2}$$

where P is the discharge power [W], Q the volumetric flow rate [m^3 s^{-1}], C_{p} and ρ being the specific heat [J kg^{-1} K^{-1}] and density [kg m^{-3}] of air, respectively. A maximum theoretical temperature increase of 51 K is determined for the investigated

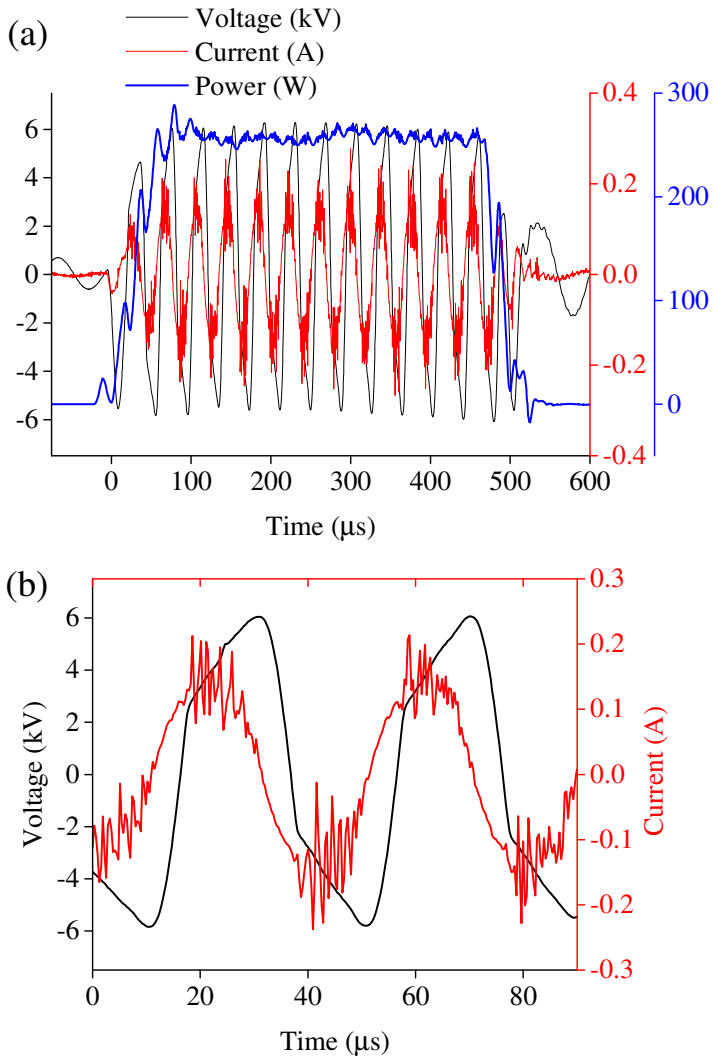

Figure 4. (a) Current, voltage and power waveforms of the DBD operated at 50% modulation at a time-averaged power of 129 W in air with a flow rate of 118 slm including aerosolization of the PRRS virus. (b) Zoom in of the current and voltage waveforms.

operating conditions of the plasma. However, upon aerosolization of the PRRS virus in the airstream, the temperature of the gas increased by only ∼20 K from the ambient room temperature corresponding to the maximum discharge power of 129 W used in this study as shown in **Figure 5**. The operating conditions of temperature and relative humidity after sampling times of 5 and 10 minutes are shown in Figure 5. Since the rate of aerosolization is constant and the air has similar moisture content at any given

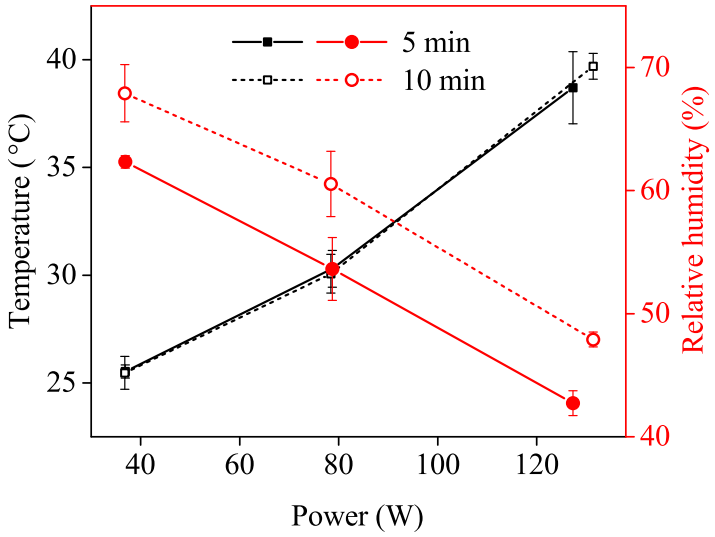

Figure 5. Conditions of temperature and relative humidity inside the wind tunnel during the operation of the DBD reactor at different discharge powers. The temperature and relative humidity inside the wind tunnel before the start of the discharge without aersolization of PRRS virus were 24°C and 24.7%, respectively.

time for a fixed sampling period during the experiment, the relative humidity decreases with the increase in temperature or power. For a sampling period of 10 minutes, the moisture content in the air is larger as compared to a 5-minute sampling period and hence the relative humidity is larger.

The observed half-life of PRRS virus reported in literature within these experimental conditions of temperature and relative humidity is in the order of several minutes,[15] which is much larger than the virus contact time of ∼3 s in this study. Thus, it is concluded that the experimental conditions cannot cause any observed PRRS virus inactivation.

3.2. PRRS virus inactivation

The infective and total PRRS virus titers were assayed by taking samples from the impingers located upstream and downstream of the DBD reactor before and after the plasma treatment by following the procedures described earlier in sections 2.3 and 2.4, and are reported in units of $\log_{10}$ $TCID_{50}$ ml^{-1} and gc ml^{-1}. For the purpose

of comparison, the virus quantification using the assay method and RT-qPCR is shown in the same plot (**Figure 6**) for a discharge power of 36.9 W and sampling time of 5 minutes. The initial virus titer in the nebulizer before aerosolization is 5.5 $\log_{10}$ $TCID_{50}$ ml^{-1}, which reduces to 3.67 $\log_{10}$ during the control experiment when sampled upstream of the DBD reactor at a flow rate of 127 slm. A further 0.24 $\log_{10}$ reduction occurs across the DBD reactor when there is no discharge. The RT-qPCR results, which quantify the total concentration of virus, show a reduction of 1.41 $\log_{10}$ gc ml^{-1} from the nebulizer (just before the treatment) to the upstream impinger, and a 0.32 $\log_{10}$ reduction in the gene copy concentrations across the reactor when there is no discharge. The 1.83 $\log_{10}$ reduction in the virus titer sampled between the nebulizer and the upstream impinger is mainly due to dilution effects. Several studies reported that the aerosolization or nebulization process does not have effect on the virus viability.[71–73] For a sampling time of 5 minutes, only 7.6% of the air containing virus aerosols is collected in the upstream impinger. The sampled solution is additionally diluted in 18 ml of DMEM solution, and only 5.9% of the solution is analyzed, which leads to a reduction in the virus titer by 1.5 orders of magnitude. Other possible reasons include loss during the process of atomization by forming larger droplets and getting settled on the bottom of the duct before reaching the upstream impinger, and/or losses to the wall along the long duct or the inside wall of the isokinetic probe. The further 0.24 $\log_{10}$ reduction in the virus titer across the DBD reactor is most likely due to the physical filtration of the virus on the inside walls of the DBD reactor.

When the DBD is operating, a similar trend is observed in the virus titer (2.0 $\log_{10}$ $TCID_{50}$ ml^{-1} reduction) and gene copy concentrations (1.5 $\log_{10}$ gc ml^{-1}) sampled between the nebulizer and the upstream impinger, confirming that the sampling at these locations is independent of the discharge. However, samples collected in the downstream impinger contain infective virus concentrations below the level of detection of the assay method (0.5 $\log_{10}$ $TCID_{50}$ ml^{-1}). Only a slight reduction (0.94 $\log_{10}$ gc ml^{-1}) is observed in the gene copy concentrations at this sampling location, while $\sim$3.5 $\log_{10}$ reduction in

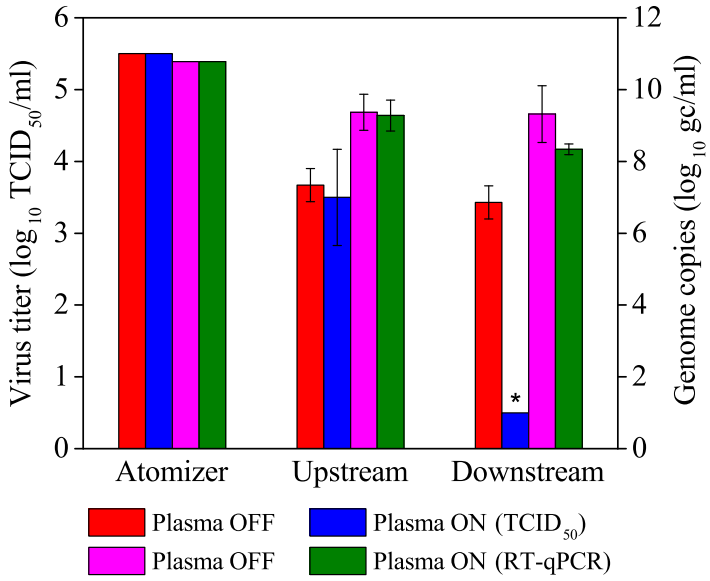

Figure 6. PRRS virus inactivation using $TCID_{50}$ assay method and RT-qPCR at sampling time of 5 minutes and discharge power of 39.6 W. $*$ denotes the limit of detection of the assay method.

the virus titer was found. This suggests that most of the PRRS virus was inactivated by the discharge, with a very small amount of virus physically removed by the DBD.

The inactivation of PRRS virus by the DBD reactor was studied for 37, 79 and 129 W, at a fixed volumetric airflow rate of 118 slm across the DBD reactor. The inactivation results of infective and total PRRS virus pertaining to 5 and 10 minutes of sampling at different discharge powers are shown in **Figure 7** and **Figure 8**, respectively. For all the investigated conditions, the virus titer in the downstream impinger is below the detection limit of the virus assay method of 0.5 $\log_{10}$ $TCID_{50}$ ml^{-1}. The small difference in the genome copy concentrations between upstream and downstream sampling as shown in Figure 8 confirms that most of the virus was inactivated independent of discharge power.

3.3. Reactive species

3.3.1. Effect of UV The effect of UV has not been investigated in this study, however, it has been reported that for complete inactivation of the PRRS virus on common farm surfaces and materials, an irradiation time of 10 minutes by UV light is required.[74]

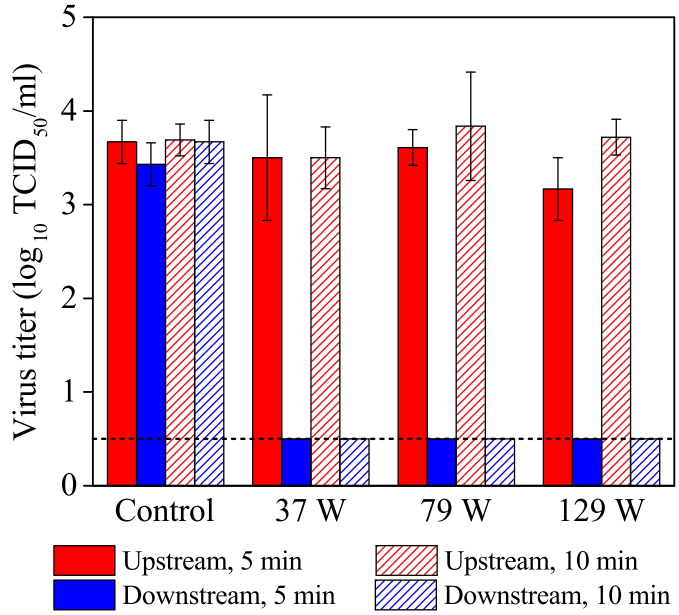

Figure 7. PRRS virus inactivation using $TCID_{50}$ assay method for sampling time of 5 minutes and 10 minutes as a function of discharge power. The dashed horizontal line represents the detection limit for the assay method.

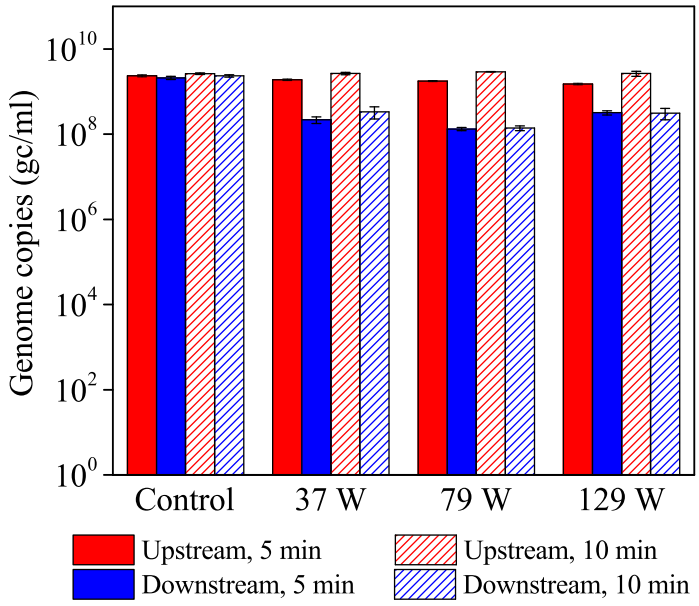

Figure 8. PRRS virus genome quantification using RT-qPCR for sampling time of 5 minutes and 10 minutes as a function of power.

This is four orders of magnitude longer than the time the virus is exposed to the UV generated by the DBD in this study. Hence, it is concluded that the effect of UV on PRRS virus is insignificant in this study.

3.3.2. Virus-laden droplets Although virus particles can exist as a single entity in air, most virus particles tend to associate with larger particles and aggregate rapidly depending on the size distribution of the aerosolized particles, the aerosol concentration and the thermodynamic conditions.[75–77] This binding or aggregation might happen by diffusion, impaction or interception.[78] The PRRS virus-laden aerosols generated by the nebulizer in this study are influenced by the size of the original droplet created by the nebulizer.[77] Most of these PRRS virus-laden droplets are a few μm in size as measured by Alonso et al using the Andersen cascade impactor.[7] These droplets are a complex mixture of the DMEM proteins in which the virus is suspended and the virus particles themselves. The airborne particle size is not governed by the size of the PRRS virus particle, which is 50–72 nm,[79] but by the size of the liquid droplet it is associated with. The size of the droplets containing PRRS virus depends on the relative humidity as well as the temperature of the air inside the wind tunnel.[77] The μm-sized virus-laden droplets can lead to faster accumulation and larger concentrations of reactive species in the droplets compared to bulk water due to the larger surface-to-volume ratio. This can drastically change the interaction of the reactive species generated by the plasma with the droplet. As the penetration depth of radicals is similar to the droplet radius,[80] both short as well as long-lived species can be important. Both are discussed separately below in more detail.

3.3.3. Long-lived species The discharge power density for this investigation corresponds well with the modeling results reported by Soloshenko et al for similar conditions of air temperature (300–500 K) and relative humidity (20–80%).[81] The dominant reactive species in the discharge afterglow, based on these models and experiments, are reactive oxygen and nitrogen species (RONS), including O_3, H_2O_2, NO, NO_2, N_2O, N_2O_5, NO_3,

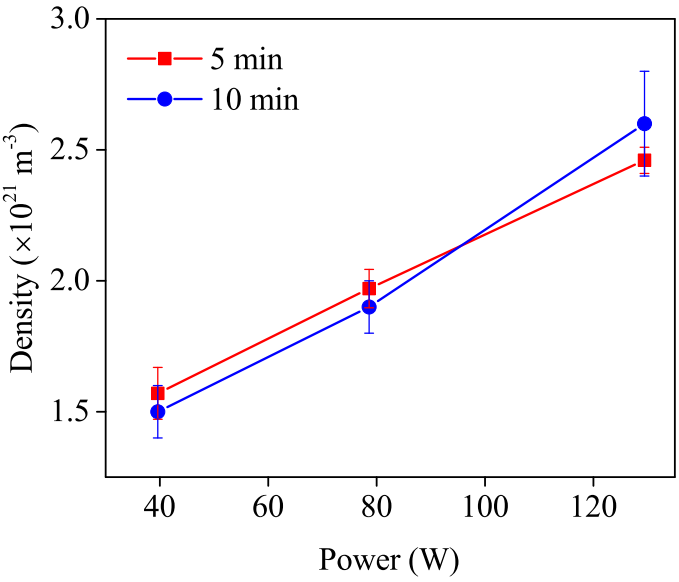

Figure 9. Gas phase ozone density measured as a function of power in air at 118 slm (for details see text).

HNO_2/NO_2^- and HNO_3/NO_3^-.

The gas-phase density of O_3 is measured using the method described in section 2.6 without aerosolization of the virus but in similar relative humidity conditions. The O_3 concentrations are shown in **Figure 9**. Although O_3 is known to have virucidal attributes, research has shown that the inactivation of PRRS virus with O_3 might take upto 10 minutes.[82] Since in the discharge afterglow, the virus aerosols are in contact with O_3 for only ∼3 s before getting collected in the downstream impinger, it can be concluded that the inactivation of the aerosolized virus observed is most likely not due to O_3. This is further supported by recent results from surface decontamination using a flow-through DBD reactor reporting that the time for complete inactivation of FCV by similar concentration of O_3 is 3 minutes. The obtained *Ct*-value (the product of concentration of the species and contact time) for 3 $\log_{10}$ reduction was 0.82 mg min l^{-1}.[51] The upper limit on the *Ct*-value of the current study is 0.023 mg min l^{-1}, which is ∼35 times smaller.

The long-lived gas-phase RNS produced by the DBD reactor such as NO, NO_2, NO_3,

N_2O and N_2O_5 would ultimately form HNO_2/NO_2^- and HNO_3/NO_3^- upon dissolution into liquid droplets.[54,83] Various studies have reported inactivation of viruses such as MS2 bacteriophage and FCV in bulk liquid by long-lived species with treatment times in the order of several minutes.[50,84] In contrast, the smaller droplets, owing to their large surface-to-volume ratio, could facilitate faster accumulation of long-lived species, and thus, achieve much higher concentrations on shorter time-scales as compared to the bulk. For instance, the liquid-phase concentration of H_2O_2 in the downstream impinger, as measured using the method described in section 2.7, is found to be quite low (< 30 μM). However, this is not representative of the concentration of H_2O_2 inside the plasma-activated aerosols or droplets. Due to a large Henry's law constant, the droplet could hold much larger concentrations of H_2O_2.[85] For a droplet diameter of 10 μm, the maximum concentration of H_2O_2 in the droplet as estimated by a model for similar conditions as used for our experiments is $\sim$200μM after 1 ms, while the accumulated concentration could be as high as 2.5 mM in an afterglow period of 3 s.[85] However, this concentration is still much smaller than the reported concentrations required for the inactivation of different viruses using H_2O_2 in bulk liquid for considerably larger treatment times.[50,84] This also eliminates H_2O_2 as a probable inactivating agent.

The liquid-phase concentrations of NO_2^- and NO_3^- in the impinger are measured as described in section 2.8 and are shown in **Figure 10(a)** and **Figure 10(b)**, respectively, as a function of sampling time for different discharge powers. The small concentration of NO_2^- was measured due to rapid oxidation of NO_2^- to NO_3^- by O_3. The slopes of the linear region of these concentration profiles provide the production rates of NO_2^- and NO_3^-. For instance, the highest production rates for NO_2^- and NO_3^- are 2.3×10^{15} s^{-1} and 3.6×10^{16} s^{-1}, respectively, for the highest discharge power of 129 W. Considering the sampling flow rate of 9 slm in the downstream impinger and assuming that all gas phase HNO_2 and HNO_3 are dissolved, the gas-phase densities of HNO_2 and HNO_3 are estimated to be 1.6×10^{19} m^{-3} and 2.4×10^{20} m^{-3}, respectively. These densities are most likely a lower limit. However, these estimated gas-phase densities are in excellent

agreement with those obtained in the modeling results for a humid air plasma containing a single water droplet.[85]

Despite large concentrations measured in this work, HNO_3 or NO_3^- do not exhibit any virucidal properties, while NO_2^- is known to possess virucidal attributes at low pH.[50,51] With increasing power, the pH of the sampled DMEM solution decreases as shown in **Figure 11**. Indeed, this drop in pH would be highly pronounced in smaller droplets as is modeled by Kruszelnicki et al,[85] which showed that the pH in the plasma-activated aerosols or droplets could be as low as 1.5 for a 10 μm droplet. In such acidic environment (pH <3.5), NO_2^- is converted into HNO_2, which can further decompose to form acidified nitrites ($^{\cdot}NO$ and $^{\cdot}NO_2$), which have bactericidal attributes.[54] The modeling study reports HNO_2 concentrations but lower than those reported by Nayak et al leading to FCV inactivation.[51]

In addition, such low pH could also stimulate the peroxynitrous acid (ONOOH) chemistry in the plasma-treated droplets known for its bactericidal and virucidal effects.[50,54] Although ONOOH has a relatively small half-life ($\sim$1 μs) compared to other long-lived species,[50] it is produced by the reaction of long-lived plasma-generated species, H_2O_2 and NO_2^-, under low pH conditions (pH $\leq$3.4) via reaction (3)[86]

$$NO_2^- + H_2O_2 + H^+ \rightarrow ONOOH + H_2O. \quad (3)$$

Kruszelnicki et al showed that the pH in the plasma-activated droplets with diameter in the range of 1 to 100 μm ranges from 0.4 to 2.2.[85] The same study also predicted the concentration of ONOOH produced in a 10 μm droplet to be 100 μM similar to estimated concentrations required for FCV inactivation.[50] Thus, long-lived species, such as peroxynitrous acid (ONOOH), could play a role in the inactivation of PRRS virus-laden liquid droplets with acidic pH (<3.1) in the effluent of the plasma.

3.3.4. Short-lived species As the virus-laden droplets are in direct contact with the plasma, the influx of the short-lived species into the droplet during the active discharge would be much higher as compared to remote or indirect treatments. Due to the short

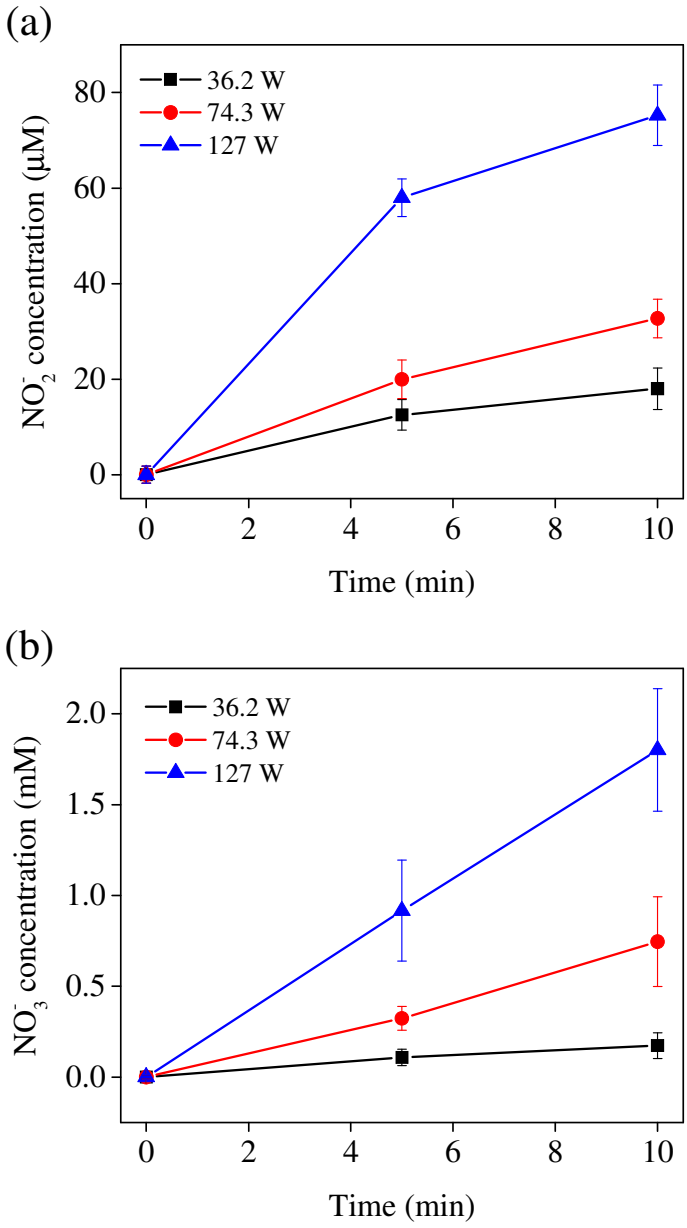

Figure 10. Liquid-phase concentrations of (a) NO_2^-, and (b) NO_3^- of solution in the impinger as a function of sampling time at different discharge powers. The measurement was performed by aerosolizing the DMEM solution without PRRS virus and sampling downstream of the DBD reactor in the impinger containing 20 ml of distilled water.

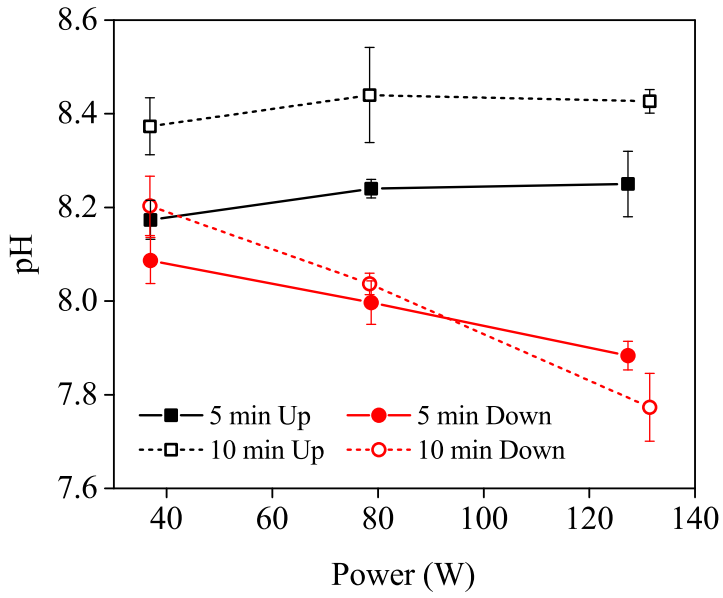

Figure 11. The pH of the DMEM solution (without virus) sampled in the impinger upon aerosolization upstream and downstream of the DBD reactor for sampling times of 5 and 10 minutes at different discharge powers.

residence time of virus aerosols in the discharge and the afterglow, the role of short-lived reactive species in the inactivation mechanism might become imperative. The short-lived species produced in a humid air micro-discharge not discussed above are electrons, positive and negative ions and radicals such as $O^{\cdot}$, $N^{\cdot}$, $H^{\cdot}$, $O_2^{\cdot -}$, $^{\cdot}OH$, $HO_2^{\cdot}$ and electronically excited molecules such as $O_2(a^1\Delta_g)$, and are present in high concentrations in the gas phase during the period of active plasma. The large surface-to-volume ratio of the virus-laden micro-droplets allows faster diffusion and accumulation of these short-lived species into the droplets.

As an example, the hydroxyl radical ($^{\cdot}OH$) is a much stronger oxidant and has a larger reduction potential as compared to O_3. Even the reaction rate constants of $^{\cdot}OH$ with organic compounds are more than 5 orders of magnitude higher than that of O_3.[87] The concentration of $^{\cdot}OH$ in the liquid droplet is limited by its penetration depth, which is tens of μm.[80] Since the size of the droplets is of similar order of magnitude, $^{\cdot}OH$ could penetrate and treat the entire droplet. This suggests that the effect of $^{\cdot}OH$ on

virus inactivation could be much higher compared to that of O_3 or any other long-lived species. The $^{\cdot}OH$ density in humid air DBD could be in the range of $10^{18} - 10^{19}$ m^{-3} within the active discharge zone, while after solvation in the plasma-activated droplets of few μm sizes, the concentration could be as high as 2 μM during the plasma on duration,[85] and might contribute to the inactivation of PRRS virus significantly.

During the first few ns of the discharge, the electrons quickly solvate into the droplet. Due to the reduction in their mobility, they could penetrate to only a few nm into the droplet. Although the solvated electrons are most likely not directly involved in the inactivation of virus, they certainly are a significant source of superoxide ions ($O_2^{\cdot -}$) due to their attachment to the dissolved oxygen in the droplet. This has been shown to enable the plasma-based $O_2^{\cdot -}$ inactivation of bacteria.[88] However, the effect of $O_2^{\cdot -}$ against virus is suggested to be through mechanism involving $ONOO^-$ through reaction with NO at anticipated acidic conditions in the plasma-treated droplets.[89,90] Thus, $O_2^{\cdot -}$ may not be a major contributor in the inactivation of PRRS virus.

A recent study reported that singlet oxygen ($O_2(a^1\Delta_g)$) produced by an Ar + 1% O_2 plasma jet contributed significantly to the inactivation of FCV in liquid solution for a short treatment time of 15 s[50] and is also a likely candidate for the PRRS virus inactivation in droplets. Similarly, $O_2(a^1\Delta_g)$ produced by a surface DBD with concentration up to $\sim$150 μM was able to inactivate bacteriophage T4 in water.[91] Given that enveloped viruses (e.g. PRRS virus) are more susceptible to the virucidal effects of $O_2(a^1\Delta_g)$ than non-enveloped viruses (such as FCV), this can lead to faster oxidation and/or disintegration of lipoprotein bilayer as well as possible modification of capsid proteins and envelope of the PRRS virus.[50]

In summary, above estimates suggest that the effect of short-lived species on inactivation of the PRRS virus likely enables the observed fast inactivation but requires additional research for a more quantitative assessment.

4. Conclusion

In this work, we showed that a volumetric DBD was effective at inactivating aerosolized PRRS virus in a wind tunnel within a few milliseconds, timescales relevant for typical HVAC conditions. A 3.5 $\log_{10}$ reduction in the viable PRRS virus titer was achieved and the inactivation effect was independent of the discharge power and the sampling time used in the study. The virus quantification by RT-qPCR showed that most of the inactivated virus RNA was captured in the sampling liquid, while only a small portion of the virus was removed by physical filtration inside the DBD reactor. The sampling time, the measured concentrations of long-lived reactive species and the pH of the sampled liquid suggested that O_3 and H_2O_2 do not play a direct role in the inactivation of aerosolized virus, while estimates based on a previous reported modeling study showed that ONOOH could initiate specific pathways to have a virucidal effect in the effluent of the discharge. Most likely, virus inactivation during in situ droplet treatment is further enhanced by short-lived species such as $^{\cdot}OH$ and $O_2(a^1\Delta_g)$.

Acknowledgments

This material is based upon work supported by the University of Minnesota and the National Science Foundation under Grant No. PHY 1903151. P. J. B. acknowledges Prof. Min Suk Cha for kindly providing the DBD electrode system. The authors thank My Yang for preparing and providing the PRRS virus strain. S. M. G. and H. A. A. acknowledge Tracy L. Otterson, PCR Lab of Minnesota VDL, for kindly providing the standard cDNA transcript of ORF6 of PRRS virus genome. G. N. gratefully acknowledges support from the Kermit and Ione Ebeltoft Interdisciplinary Doctoral Fellowship and the technical assistance of Ankit Moldgy and Wei Xiao.

References

[1] Nieuwenhuis N, Duinhof T and Van Nes A 2012 *Vet. Rec.* 1–4

[2] Neumann E J, Kliebenstein J B, Johnson C D, Mabry J W, Bush E J, Seitzinger A H, Green A L and Zimmerman J J 2005 *J. Am. Vet. Med. A.* **227** 385–392

[3] Green J L 2015 Update on the highly-pathogenic avian influenza outbreak of 2014-2015

[4] Bender J B, Hueston W and Osterholm M 2006 *J. Agromedicine* **11** 5–15

[5] Pileri E and Mateu E 2016 *Vet. Res.* **47** 108

[6] Nor M M, Gan C and Ong B 2000 *Rev. Sci. Tech. OIE* **19** 160–165

[7] Alonso C, Raynor P C, Goyal S, Olson B A, Alba A, Davies P R and Torremorell M 2017 *J. Vet. Diagn. Investig.* **29** 298–304

[8] Alonso C, Raynor P C, Davies P R, Morrison R B and Torremorell M 2016 *Aerobiologia* **32** 405–419

[9] Alonso C, Davies P R, Polson D D, Dee S A and Lazarus W F 2013 *Prev. Vet. Med.* **111** 268–277

[10] Alonso C, Goede D P, Morrison R B, Davies P R, Rovira A, Marthaler D G and Torremorell M 2014 *Vet. Res.* **45** 73

[11] Otake S, Dee S, Corzo C, Oliveira S and Deen J 2010 *Vet. Microbiol.* **145** 198–208

[12] Anderson B D, Lednicky J A, Torremorell M and Gray G C 2017 *Front. Vet. Sci.* **4** 121

[13] Torremorell M, Alonso C, Davies P R, Raynor P C, Patnayak D, Torchetti M and McCluskey B 2016 *Avian Dis.* **60** 637–643

[14] Jonges M, Van Leuken J, Wouters I, Koch G, Meijer A and Koopmans M 2015 *PLoS One* **10** e0125401

[15] Hermann J, Hoff S, Muñoz-Zanzi C, Yoon K J, Roof M, Burkhardt A and Zimmerman J 2007 *Vet. Res.* **38** 81–93

[16] Tousignant S J, Perez A M, Lowe J F, Yeske P E and Morrison R B 2015 *Am. J. Vet. Res.* **76** 70–76

[17] Ontario H Q *et al.* 2005 *Ont. Health Technol. Assess. Ser.* **5** 1

[18] EPA Indoor Environments Division 2018 Residential air cleaners – a technical summary Tech. rep. U.S. Environmental Protection Agency

[19] Park G, Linden K and Sobsey M 2011 *Lett. Appl. Microbiol.* **52** 162–167

[20] Nuanualsuwan S, Mariam T, Himathongkham S and Cliver D O 2002 *Photochem. Photobiol.* **76** 406–410

[21] Thurston-Enriquez J A, Haas C N, Jacangelo J, Riley K and Gerba C P 2003 *Appl. Environ. Microbiol.* **69** 577–582

[22] de Roda Husman A M, Bijkerk P, Lodder W, Van Den Berg H, Pribil W, Cabaj A, Gehringer P, Sommer R and Duizer E 2004 *Appl. Environ. Microbiol.* **70** 5089–5093

[23] Wells W F and Fair G M 1935 *Science* **82** 280–281

[24] Wells W and Brown H 1936 *Am. J. Epidemiol.* **24** 407–413

[25] Kowalski W and Bahnfleth W P 2000 *Heat. Piping Air Cond.* **72**

[26] Scheir R and Fencl F B 1996 *Heat. Piping Air Cond.* **68**

[27] VanOsdell D and Foarde K 2002 Defining the effectiveness of uv lamps installed in circulating air ductwork Tech. rep. Air-Conditioning and Refrigeration Technology Institute, Arlington, VA (US); RTI International, Research Triangle Park, NC (US)

[28] Hijnen W, Beerendonk E and Medema G J 2006 *Water Res.* **40** 3–22

[29] Lytle C 1971 *Int. J. Radiat. Biol. Relat. Stud. Phys. Chem. Med.* **19** 329–337

[30] Morawska L, Agranovski V, Ristovski Z and Jamriska M 2002 *Indoor Air* **12** 129–137

[31] Wallace L A, Emmerich S J and Howard-Reed C 2004 *Atmos. Environ.* **38** 405–413

[32] Howard-Reed C, Wallace L A and Emmerich S J 2003 *Atmos. Environ.* **37** 5295–5306

[33] Guan T and Yao M 2010 *J. Aerosol Sci.* **41** 611–620

[34] Xu Z and Yao M 2011 *J. Aerosol Sci.* **42** 387–396

[35] Grinshpun S A, Adhikari A, Honda T, Kim K Y, Toivola M, Ramchander Rao K and Reponen T 2007 *Environ. Sci. Technol.* **41** 606–612

[36] Jung J H, Lee J E, Lee C H, Kim S S and Lee B U 2009 *Appl. Environ. Microbiol.* **75** 2742–2749

[37] Johansson E, Adhikari A, Reponen T, Yermakov M and Grinshpun S A 2011 *Aerosol Sci. Technol.* **45** 376–381

[38] Wu Y and Yao M 2010 *J. Aerosol Sci.* **41** 682–693

[39] Zhang Q, Damit B, Welch J, Park H, Wu C Y and Sigmund W 2010 *J. Aerosol Sci.* **41** 880–888

[40] Laroussi M 2002 *IEEE Plasma Sci.* **30** 1409–1415

[41] Ma R, Wang G, Tian Y, Wang K, Zhang J and Fang J 2015 *J. Hazard. Mater.* **300** 643–651

[42] Scholtz V, Pazlarova J, Souskova H, Khun J and Julak J 2015 *Biotechnol. Adv.* **33** 1108–1119

[43] Misra N, Tiwari B, Raghavarao K and Cullen P 2011 *Food Eng. Rev.* **3** 159–170

[44] Laroussi M 2005 *Plasma Process. Polym.* **2** 391–400

[45] Kong M G, Kroesen G, Morfill G, Nosenko T, Shimizu T, Van Dijk J and Zimmermann J 2009 *New J. Phys.* **11** 115012

[46] Mizuno A 2000 *IEEE Trans. Dielectr. Electr. Insul.* **7** 615–624

[47] Graves D B 2012 *J. Phys. D: Appl. Phys.* **45** 263001

[48] Fridman G, Brooks A D, Balasubramanian M, Fridman A, Gutsol A, Vasilets V N, Ayan H and Friedman G 2007 *Plasma Process. Polym.* **4** 370–375

[49] Moreau M, Orange N and Feuilloley M 2008 *Biotechnol. Adv.* **26** 610–617

[50] Aboubakr H A, Gangal U, Youssef M M, Goyal S M and Bruggeman P J 2016 *J. Phys. D: Appl. Phys.* **49** 204001

[51] Nayak G, Aboubakr H A, Goyal S M and Bruggeman P J 2018 *Plasma Process. Polym.* **15** 1700119

[52] Pavlovich M J, Clark D S and Graves D B 2014 *Plasma Sources Sci. Technol.* **23** 065036

[53] Machala Z, Chládeková L and Pelach M 2010 *J. Phys. D: Appl. Phys.* **43** 222001

[54] Lukes P, Dolezalova E, Sisrova I and Clupek M 2014 *Plasma Sources Sci. Technol.* **23** 015019

[55] Aboubakr H A, Williams P, Gangal U, Youssef M M, El-Sohaimy S A, Bruggeman P J and Goyal S M 2015 *Appl. Environ. Microbiol.* **81** 3612–3622

[56] Wende K, Williams P, Dalluge J, Van Gaens W, Aboubakr H, Bischof J, Von Woedtke T, Goyal S M, Weltmann K D, Bogaerts A, Masur K and Bruggeman P J 2015 *Biointerphases* **10** 029518

[57] Zimmermann J L, Dumler K, Shimizu T, Morfill G, Wolf A, Boxhammer V, Schlegel J, Gansbacher B and Anton M 2011 *J. Phys. D: Appl. Phys.* **44** 505201

[58] Xia T, Kleinheksel A, Lee E, Qiao Z, Wigginton K and Clack H 2019 *J. Phys. D: Appl. Phys.* **52** 255201

[59] Wu Y, Liang Y, Wei K, Li W, Yao M, Zhang J and Grinshpun S A 2015 *Appl. Environ. Microbiol.* **81** 996–1002

[60] Terrier O, Essere B, Yver M, Barthélémy M, Bouscambert-Duchamp M, Kurtz P, VanMechelen D, Morfin F, Billaud G, Ferraris O, Lina B, Rosa-Calatrava M and Moules V 2009 *J. Clin. Virol.* **45** 119–124

[61] Uhm H S, Lee K H and Seong B L 2009 *Appl. Phys. Lett.* **95** 173704

[62] Hudson J B, Sharma M and Vimalanathan S 2009 *Ozone Sci. Eng.* **31** 216–223

[63] Hudson J, Sharma M and Petric M 2007 *J. Hosp. Infect.* **66** 40–45

[64] Cha M, Song Y, Lee J and Kim S 2007 *Int. J. Environ. Sci. Technol.* **1** 28–33

[65] Nayak G, Du Y, Brandenburg R and Bruggeman P J 2017 *Plasma Sources Sci. Technol.* **26** 035001

[66] Kärber G 1931 *Naunyn-Schmiedeberg's Arch. Pharmacol.* **162** 480–483

[67] Aboubakr H A, Mor S K, Higgins L, Armien A, Youssef M M, Bruggeman P J and Goyal S M 2018 *PloS One* **13** e0194618

[68] Nayak G, Sousa J S and Bruggeman P J 2017 *J. Phys. D: Appl. Phys.* **50** 105205

[69] Eisenberg G 1943 *Ind. Eng. Chem., Anal. Ed.* **15** 327–328

[70] Miranda K M, Espey M G and Wink D A 2001 *Nitric Oxide* **5** 62–71

[71] Zuo Z, Kuehn T H, Verma H, Kumar S, Goyal S M, Appert J, Raynor P C, Ge S and Pui D Y 2013 *Aerosol Sci. Tech.* **47** 373–382

[72] Kim S W, Ramakrishnan M, Raynor P C and Goyal S M 2007 *Aerobiologia* **23** 239–248

[73] Ijaz M, Karim Y, Sattar S and Johnson-Lussenburg C 1987 *J. Virol. Methods* **18** 87–106

[74] Dee S, Otake S and Deen J 2011 *Vet. Microbiol.* **150** 96–99

[75] Stölzel M, Breitner S, Cyrys J, Pitz M, Wölke G, Kreyling W, Heinrich J, Wichmann H E and Peters A 2007 *J. Expo. Sci. Environ. Epidemiol.* **17** 458

[76] Hogan Jr C, Kettleson E, Lee M H, Ramaswami B, Angenent L and Biswas P 2005 *J. Appl. Microbiol.* **99** 1422–1434

[77] Verreault D, Moineau S and Duchaine C 2008 *Microbiol. Mol. Biol. Rev.* **72** 413–444

[78] Hinds W C 1999 *Aerosol Technology: Properties, Behavior, and Measurement of Airborne Particles* (John Wiley & Sons)

[79] Dea S, Gagnon C, Mardassi H, Pirzadeh B and Rogan D 2000 *Arch. Virol.* **145** 659–688

[80] Chen C, Liu D, Liu Z, Yang A, Chen H, Shama G and Kong M 2014 *Plasma Chem. Plasma Process.* **34** 403–441

[81] Soloshenko I, Tsiolko V, Pogulay S, Kalyuzhnaya A, Bazhenov V Y and Shchedrin A 2009 *Plasma Sources Sci. Technol.* **18** 045019

[82] Yoon Y D and Kim W I 2013 *Korean J. Vet. Res.* **36** 157–162

[83] Kimura Y, Takashima K, Sasaki S and Kaneko T 2018 *J. Phys. D: Appl. Phys.* **52** 064003

[84] Pottage T, Richardson C, Parks S, Walker J and Bennett A 2010 *J. Hosp. Infect.* **74** 55–61

[85] Kruszelnicki J A, Lietz A M and Kushner M J 2019 *J. Phys. D: Appl. Phys.* **52** 355207

[86] Robinson K M and Beckman J S 2005 *Methods Enzymol.* **396** 207–214

[87] Huie R E 2003 *Journal of Research (NIST JRES)-* **108**

[88] Kondeti V S S K, Phan C Q, Wende K, Jablonowski H, Gangal U, Granick J L, Hunter R C and Bruggeman P J 2018 *Free Radic. Biol. Med.* **124** 275–287

[89] Akaike T, Suga M and Maeda H 1998 *Proc. Soc. Exp. Biol. Med.* **217** 64–73

[90] Pryor W A and Squadrito G L 1995 *Am. J. Physiol. Lung Cell Mol. Physiol.* **268** L699–L722

[91] Guo L, Xu R, Gou L, Liu Z, Zhao Y, Liu D, Zhang L, Chen H and Kong M G 2018 *Appl. Environ. Microbiol.* **84** e00726–18

Graphical Abstract

Aerosolized porcine reproductive and respiratory syndrome virus in a wind tunnel are inactivated by a flow-through volumetric dielectric barrier discharge with a gas residence time of 15 milliseconds. A $\sim$3.5 $\log_{10}$ reduction in the virus titer is achieved. An analysis of the results partially based on previously reported modeling of plasma aerosol treatments suggest that both short-lived and long-lived reactive species can be responsible for the observed inactivation.

G. Nayak, A. J. Andrews, I. Marabella, H. A. Aboubakr, S. M. Goyal, B. A. Olson, M. Torremorell, P. J. Bruggeman*

Rapid inactivation of airborne porcine reproductive and respiratory syndrome (PRRS) virus using an atmospheric pressure air plasma